

January 06, 2012

Rules and limitations of building delay-tolerant topologies for coupled systems

Rifat Sipahi
Northeastern University

Wei Qiao
Northeastern University

Recommended Citation

Sipahi, Rifat and Qiao, Wei, "Rules and limitations of building delay-tolerant topologies for coupled systems" (2012). *Mechanical and Industrial Engineering Faculty Publications*. Paper 51. <http://hdl.handle.net/2047/d20004064>

This work is available open access, hosted by Northeastern University.

Rules and limitations of building delay-tolerant topologies for coupled systems

Wei Qiao and Rifat Sipahi*

Department of Mechanical and Industrial Engineering, Northeastern University, Boston, Massachusetts 02115

(Received 27 July 2011; published 6 January 2012)

This paper investigates the equilibrium behavior of broadly studied synchronization dynamics of coupled systems, among which shared information is delayed. The underlying relationship is established between graph structures and the largest amount of delay the dynamics can withstand without losing stability. In particular, based on Cartesian product of graphs, we present the rules and limitations for synthesizing the graphs of large-scale systems that can remain stable for as large delays as possible. Examples are provided to demonstrate the results.

DOI: [10.1103/PhysRevE.85.016104](https://doi.org/10.1103/PhysRevE.85.016104)

PACS number(s): 89.75.Fb, 02.30.Ks, 02.10.Ox, 05.45.Xt

I. INTRODUCTION

Understanding the mechanisms of synchronization dynamics of coupled systems offers opportunities in uncovering the many intricacies of biological systems [1], social networks [2], neural networks [3,4], traffic flow patterns [5–7], and supply chain networks [8]. Many studies are published along these lines, including the investigation of diffusively coupled identical systems [9–13], chaotic oscillators [14], network synchronization under noise effects [15,16], stochastic networks in fish schooling [17], effects of communication delays between coupled systems [18], and the effects of changes in graphs to Laplacian eigenvalues [19–21].

Synchronization can be achieved only if the coupled systems, also known as “nodes,” communicate with each other, become aware of each others’ moves, and accordingly make decisions toward synchronization. This, however, may not always be achievable, especially when communication links between the nodes cause information transmission delays, as found in analogous forms in neural networks, car following under human reaction delays, synchronization of autonomous agents, supply chains, and swarming [22]. Due to delays, each node can be aware of the status of the other nodes only after a certain amount of time. In one sense, delay can be seen as a limitation of how fresh the available information can be in the network. As expected, decisions made as an attempt to achieve synchronization, but that are based on *delayed* information, may drive the coupled system to instability [23], which can be seen as *nonsynchronizability*.

Nonsynchronizability in many cases is undesirable, yet there are biological systems where it can also be useful [19]. In this article, the focus is to avoid nonsynchronizability; however, the framework constructed here can be used to study the converse. Synchronizability in a coupled system with delays can be analyzed by performing stability analysis, e.g., by following the work in Refs. [24–28]. We also find studies on the eigenvalue distributions of Laplacians associated with particular graph structures [5,18,29–31]. Nevertheless, synchronizability, delays, and graph structures are all interrelated, and thus need to be studied in an ensemble [29,32,33]. This observation motivates the paper, in which we take the equilibrium behavior of a synchronization dynamics studied

broadly in the literature [15,16,18,30,31,34,35] and explain the synchronizability (stability) features of the equilibrium in connection with (i) for how much delays synchronizability can still hold and (ii) how the corresponding graph structures can be tailored while still maintaining synchronizability.

The contributions in this article stem from our recent results on the responsible eigenvalue (RE) concept [33,36]. RE establishes the relationship between the *finite* number of eigenvalues of the graph Laplacian and the *largest amount of delay* that the equilibrium dynamics can tolerate before becoming nonsynchronizable. Although the synchronizability analysis alone is *infinite dimensional* due to delays, our RE concept bypasses this analysis and simply requires checking the finite numbered Laplacian eigenvalues in order to determine the tolerable amount of delay. With RE results at hand, by utilizing Cartesian product operation on graphs [19], we can now establish rules with which large scale graphs can be designed while still maintaining sufficient tolerance against the detrimental effects of delays in the arising graphs.

The article is organized as follows. In Sec. II, we introduce preliminaries, including the coupled system under investigation, discuss the concept of responsible eigenvalue, and overview the properties of Cartesian product of graphs. In Sec. III, we present the main results, and we conclude with discussions in Sec. IV.

II. PRELIMINARIES

In this section, the synchronization dynamics under study are presented, followed by the responsible eigenvalue concept and Cartesian product of graphs.

A. Synchronization model with delay

In this article, we start with the following coupled system, where at each node $i = 1, \dots, n$ lies a first-order nonlinear dynamics,

$$\begin{aligned} \dot{y}_i(t) &= f_i(\Delta_{1,i}(t - \tau), \dots, \Delta_{n,i}(t - \tau)), \\ \Delta_{k,i}(t) &= y_k(t) - y_i(t), \quad k = 1, \dots, n, k \neq i, \end{aligned} \quad (1)$$

where $y_i(t)$ is the state of node i , nonlinear function f_i is continuous and differentiable with respect to its arguments, and τ is the positive constant delay. Here, our interest is to analyze the equilibrium dynamics of Eq. (1) in light of the objectives

*rifat@coe.neu.edu

mentioned in the previous section. For this, we linearize Eq. (1) around the constant equilibrium $\mathbf{y}^* = (y_1^*, \dots, y_n^*)^T$ found from Eq. (1) by setting all $y_i(t) = 0$, and investigate the dynamics of perturbations $x_i(t)$ around the equilibrium, $y_i^* = y_i(t) - x_i(t)$. Linearizing Eq. (1) under these conditions leads to

$$\dot{x}_i(t) = \sum_{k=1, k \neq i}^n \alpha_{ik} [x_k(t - \tau) - x_i(t - \tau)], \quad (2)$$

where the constant weights α_{ik} are the coupling strengths, which are also the entries of the Jacobian of $(f_1, \dots, f_n)^T$, denoted by \mathbf{A} and calculated at the equilibrium \mathbf{y}^* . We next write Eq. (2) in matrix form as

$$\dot{\vec{x}}(t) = \mathbf{A}\vec{x}(t - \tau), \quad (3)$$

where $\vec{x}(t) = [x_1(t), \dots, x_n(t)]^T \in \mathbb{R}^n$, and \mathbf{A} is also known as the configuration matrix [18,30].

Equations (1) and (2) have been broadly studied in the literature in the context of neural networks [4], synchronization [15,16,35], traffic flow [5,6,37], and autonomous agents [18,29–31,34,38,39]. Different than the earlier work, here we consider the graph as a parameter in the analysis of synchronization dynamics, and thus the objective here is to reveal how graphs corresponding to large dimensional \mathbf{A} could be synthesized based on the eigenvalues of \mathbf{A} , while assuring that the dynamics in Eq. (3) can withstand as large delays as possible without becoming nonsynchronizable (unstable).

Some assumptions are as follows. There exists a directed path from every node to all other nodes, although some nodes may not be sharing information with each other. Furthermore, inspecting Eq. (2) reveals that \mathbf{A} has zero row sum. It is then easy to see that \mathbf{A} with the corresponding graph G has a single zero eigenvalue [5,30]. We use the convention of denoting $\lambda_1(\mathbf{A}) = 0$ and study Eq. (3) with nonnegative coupling strengths $\alpha_{ik} \geq 0$, which also implies that $\lambda_2, \dots, \lambda_n \in \mathbb{C}_-$ [40]. Under these conditions, one can reveal from the characteristic equation found from Eq. (3) that, for all τ , the dynamics in Eq. (3) has a mode with $\beta_1 e^{\lambda_1 t}$. So long as all the other dynamic modes vanish, all $x_i(t)$ converges to β_1 as $t \rightarrow \infty$ [5,30], indicating that system in Eq. (1) synchronizes in the linear regime.

B. Synchronizability and responsible eigenvalue

Synchronizability of the equilibrium is based on the delay value τ in Eq. (3). In order to reveal the largest amount of delay that Eq. (3) can tolerate without becoming nonsynchronizable, the eigenvalues of Eq. (3) should be studied. First of all, as we confirmed, the rigid-body dynamics of Eq. (3) related to $\lambda_1 = 0$ does not influence the remaining dynamic modes of Eq. (3) [33]. For this reason, we investigate the synchronizability of Eq. (3) around its rigid body dynamics, disregarding $\lambda_1 = 0$ in the rest of the text. Due to delay, the dynamics in Eq. (3) has *infinitely many eigenvalues*, and its synchronizability is guaranteed if and only if all these eigenvalues have *negative* real parts. To be consistent with this synchronizability property, we define the *negative* Laplacian as $\mathcal{Q}(G) = -\mathcal{L}(G) = \mathbf{A}$.

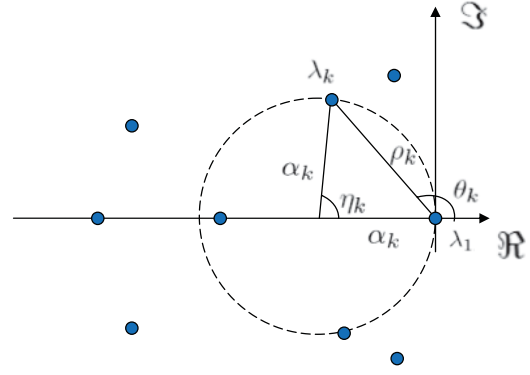


FIG. 1. (Color online) The eigenvalues of \mathbf{A} in Eq. (3), $\lambda_1 = 0$ and $\lambda_2, \dots, \lambda_n$ are in general real and complex conjugate.

For the type of dynamics in Eq. (3), it is known that there is an upper bound on the delay value, called the delay margin (threshold for synchronizability) τ^* , less than which Eq. (3) is synchronizable around its rigid body dynamics [15,16,33]. In other words, τ^* is the largest delay that Eq. (3) can tolerate before becoming nonsynchronizable.

Lemma 1. Either one real or one pair of complex conjugate eigenvalue(s) of \mathbf{A} directly determines the delay margin τ^* [33,36,41].

Proof. The proof is based on an infinite-dimensional eigenvalue analysis, and its details are left to the cited studies. In summary, it can be shown that the minimum positive delay associated with λ_k is reduced to a finite-dimensional analysis, given by

$$\tau_k^* = \frac{\eta_k/2}{2\alpha_k \sin \eta_k/2}, \quad k = 2, \dots, n, \quad (4)$$

where η_k and α_k are related to λ_k as shown in Fig. 1. We then conclude that the delay margin is

$$\tau^* = \min_{k=2, \dots, n} \tau_k^*, \quad (5)$$

which proves the lemma. \blacksquare

Note that the expression in Eq. (4) for $\lambda_k(\mathbf{A}) \in \Re$ leads to $\tau \cdot \max_{k=2, \dots, n} |\lambda_k| < \frac{\pi}{2}$ for synchronizability condition, which is consistent with the results in Refs. [15,18]. Here, Lemma 1 extends the case of $\lambda_k(\mathbf{A}) \in \Re$ to the case of complex eigenvalues $\lambda_k(\mathbf{A}) \in \mathbb{C}$. In our recent work [33,36,41], we call the particular eigenvalue of \mathbf{A} that minimizes τ_k^* in Eq. (5) as the responsible eigenvalue denoted by RE. The advantage of RE is that it is either one of the real or one of the complex conjugate eigenvalue(s) of \mathbf{A} . In this regard, knowing the graph G of Eq. (3) directly allows identifying τ^* , surpassing the need to know the *infinitely* many eigenvalues of Eq. (3).

Using Eq. (4), one can now back-calculate the locations of λ_k , for which τ_k^* remains fixed. This leads to the delay margin contour map (DMCM) in Fig. 2. On this map, one can superpose all λ_k of \mathbf{A} and identify λ_k that resides on the contour with the *smallest contour value*. This is the responsible eigenvalue, and τ^* is the contour value, consistent with Eq. (5). As discussed in the next section, the geometry of the contours, which become intricate, especially for $\lambda_k(\mathbf{A}) \in \mathbb{C}$, is extremely crucial for establishing the main results of this paper.

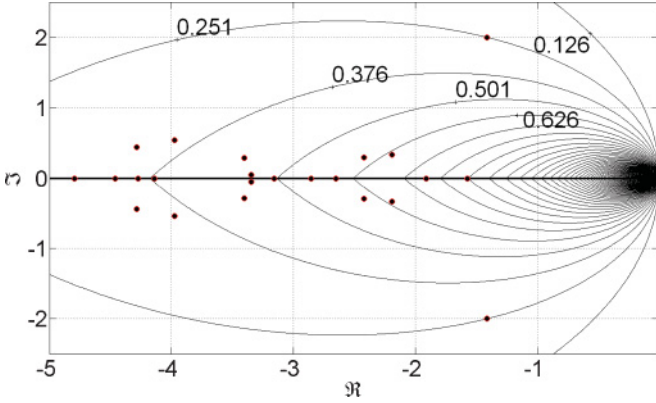


FIG. 2. (Color online) Delay margin contour map (DMCM) with superposed eigenvalues (dots) of a representative matrix \mathbf{A} . Each contour is labeled with the corresponding τ^* value. The responsible eigenvalue is the eigenvalue residing on the contour with the smallest contour value, which is $\tau^* = 0.251$ in this example.

C. Cartesian product of graphs

Lemma 2. Cartesian product [20]. Let G_1 and G_2 be graphs with n_1 and n_2 vertices, respectively. Let G_3 be the Cartesian product of G_1 and G_2 given by $G_3 = G_1 \times G_2$ (Fig. 3). Then the eigenvalues of $\mathcal{Q}(G_3)$ are all possible sums $\lambda_i[\mathcal{Q}(G_1)] + \lambda_p[\mathcal{Q}(G_2)]$, where $1 \leq i \leq n_1$ and $1 \leq p \leq n_2$.

Definition 1. The Kronecker sum [42], denoted by \oplus , is the matrix sum defined as

$$\mathcal{Q}(G_1) \oplus \mathcal{Q}(G_2) = \mathcal{Q}(G_1) \otimes I_{n_2} + I_{n_1} \otimes \mathcal{Q}(G_2), \quad (6)$$

where \otimes denotes the Kronecker product operation, the dimension of $\mathcal{Q}(G_i)$, $i = 1, 2$, is n_i , which is also the number of vertices of G_i as per (2), and I_q is the $q \times q$ identity matrix. The eigenvalues of $\mathcal{Q}(G_3)$ found from $\mathcal{Q}(G_3) = \mathcal{Q}(G_1) \oplus \mathcal{Q}(G_2)$ are all possible sums of the eigenvalues of $\mathcal{Q}(G_1)$ and $\mathcal{Q}(G_2)$. This property represents the linear algebra underlying Cartesian product operation.

Notice that Lemma 2 holds for both real and complex conjugate eigenvalues, just like the RE concept introduced above. Furthermore, if $\mathcal{Q}(G_1)$ and $\mathcal{Q}(G_2)$ have zero row sum, similar to \mathbf{A} in Eq. (3), then it is easy to show that $\mathcal{Q}(G_3)$ has zero row sum.

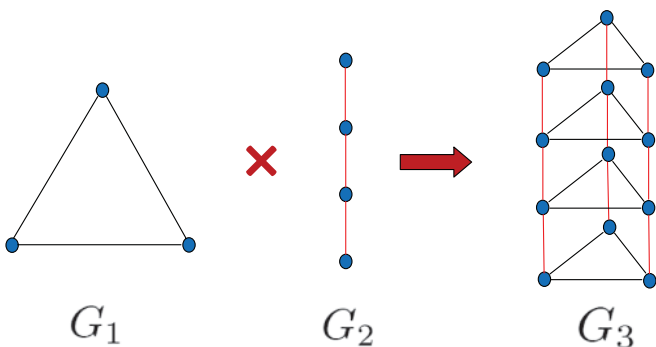


FIG. 3. (Color online) The Cartesian product of two graphs, G_1 and G_2 , is denoted by $G_3 = G_1 \times G_2$.

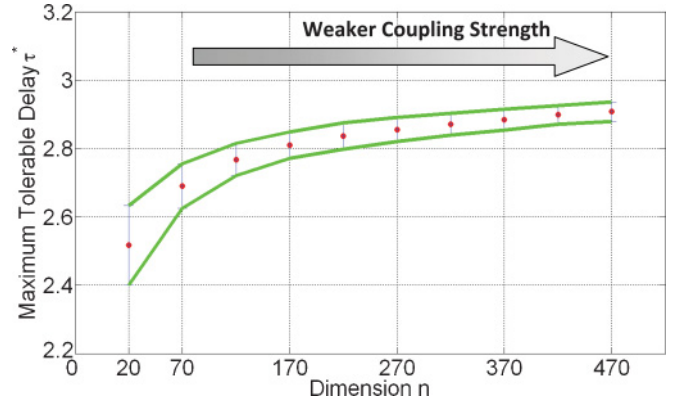


FIG. 4. (Color online) Mean and standard deviation of the delay margin τ^* with respect to the number of nodes n . All the nondiagonal entries α_{ik} , $i \neq k$, are numerically randomized, and 300 different \mathbf{A} are constructed for each n , where matrix \mathbf{A} is then scaled by $1/n$ for the calculation of τ^* .

III. MAIN RESULT

In this section, the RE concept is utilized for building arbitrarily large topologies for the dynamics in Eq. (2), such that the delay margin of the arising large-scale system can be made as large as possible.

A. Randomization of coupling strengths

Having established the correlation between τ^* and λ_k , we now randomize the nondiagonal entries of \mathbf{A} , making sure that \mathbf{A} maintains zero row sum, and study the effects of the dimension n of \mathbf{A} on τ^* . It is crucial, however, that we maintain a fixed average weighting of all the coupling strengths of each node. This allows, on average, a measure of balance between the number of nodes that a node is connected to versus the sum of all the coupling strengths due to these connections. For this purpose, we scale \mathbf{A} by $1/n$ with the assumption that all the entries of \mathbf{A} are in general nonzero under randomization. In Fig. 4, we present how τ^* changes as n grows, as we perform randomizations of all $\alpha_{ik} \in [0, 1]$, $i \neq k$, selected from a uniform distribution, and calculating τ^* as per Eq. (5) for 300 different \mathbf{A} matrices for each n value. Clearly, the trend is that the average of the delay margin τ^* is increasing as n increases. Since α_{ik} are scaled by $1/n$, this leads to weaker couplings among the nodes as n increases.¹

Three crucial observations are as follows. Weak coupling allows larger τ^* as shown in Fig. 4. This can also be proved using Gershgorin’s circle theorem [43]. We can show that, for larger n , the eigenvalues of $\frac{1}{n}\mathbf{A}$ are located in circles with smaller radii on the left-half plane nearby the origin. Inspecting Fig. 2, we can see that by encapsulating these eigenvalues in such small regions, we can increase the delay margin of the dynamics (see the contour values on DMCM). This pattern

¹As a side note, we remark that it is very likely that \mathbf{A} has distinct eigenvalues due to randomization; however, for the implementation of RE, no restrictions are imposed here, regarding whether or not \mathbf{A} has distinct or multiple eigenvalues and whether \mathbf{A} is diagonalizable or nondiagonalizable.

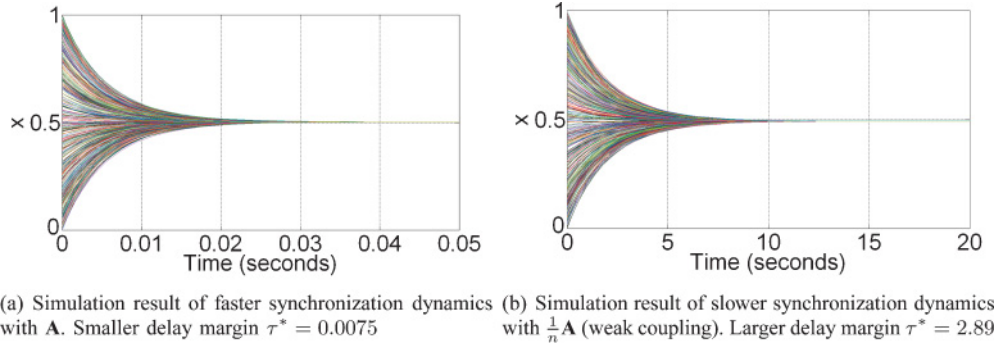


FIG. 5. (Color online) Simulation results showing the decay rate of faster and slower perturbation dynamics. $n = 370$ nodes and $\tau = 0$.

has also been revealed for the case of $\lambda(\mathbf{A}) \in \mathfrak{R}$ [15,16], and here we see that the results extend to the complex-eigenvalue case. Second observation is that, with randomization and weak coupling, we can increase the delay tolerance of the large-scale network. However, randomization does not give any clues as to how one would design a graph and the coupling strengths such that a particular delay margin of the large-scale system can be attained. We leave the details of this part to the next subsection. Third, weaker coupling pushes λ_k closer to the origin of the complex plane, thereby reducing the decay rate of the perturbations. This can also be verified via simulations of $\vec{x}(t)$; see Figs. 5(a) and 5(b). Since the focus here is not on the decay rate of $x_i(t)$, we refer the readers to Refs. [15,16,44] for analytical studies on eigenvalue distributions.

B. Tailoring graphs using Cartesian product

In this subsection, all the matrices $\mathcal{Q}(G_i)$ follow the properties of \mathbf{A} in Eq. (3), that is, the coupling strengths are positive real, $\mathcal{Q}(G_i)$ has zero row sum, G_i is connected, and $\lambda_1[\mathcal{Q}(G_i)] = 0$. Graph G_i has n_i number of nodes ($i = 1, \dots, 3$), which is also the dimension of $\mathcal{Q}(G_i)$, and the corresponding delay margin is denoted by $\tau_{G_i}^*$ found from Eq. (5) using the RE, which is one of the eigenvalues $\lambda_z[\mathcal{Q}(G_i)]$, $z = 2, \dots, n_i$. Furthermore, in this subsection, we specifically focus on combining the two graphs G_1 and G_2 using Cartesian product operation, which leads to a larger graph $G_3 = G_1 \times G_2$, where $n_3 = n_1 \cdot n_2$. Unless otherwise stated, this is the understanding in what follows.

Lemma 3. Excluding $\lambda_1 = 0$, the eigenvalues of $\mathcal{Q}(G_3)$ have negative real parts, if and only if all the nonzero eigenvalues of both $\mathcal{Q}(G_1)$ and $\mathcal{Q}(G_2)$ have negative real parts.

Proof. The proof follows from the properties of the Kronecker summation. The lemma is if and only if since $\lambda_1[\mathcal{Q}(G_1)] = \lambda_1[\mathcal{Q}(G_2)] = 0$. ■

The above lemma states that the first rule of building a large graph G_3 is to have two negative Laplacians $\mathcal{Q}(G_1)$ and $\mathcal{Q}(G_2)$ whose nonzero eigenvalues have negative real parts. This is guaranteed as we assume that all the coupling strengths are positive.

Corollary 1. Let all nonzero eigenvalues of $\mathcal{Q}(G_1)$ and $\mathcal{Q}(G_2)$ be negative real. Then the delay margin $\tau_{G_3}^*$ is less than both $\tau_{G_1}^*$ and $\tau_{G_2}^*$.

Proof. As per Definition 1, we have $\lambda_q[\mathcal{Q}(G_3)] \in \mathbb{R}_-$, $q = 2, \dots, n_1 \cdot n_2$ since $\lambda_i[\mathcal{Q}(G_1)] \leq 0$ and $\lambda_p[\mathcal{Q}(G_2)] \leq 0$. Consequently, there exist at least one $q, q \geq 2$, such

that $\lambda_q[\mathcal{Q}(G_3)] < \min\{\lambda_i[\mathcal{Q}(G_1)], \lambda_p[\mathcal{Q}(G_2)]\}$ for all $i = 2, \dots, n_1$ and $p = 2, \dots, n_2$. Inspecting Eq. (4) as well as Fig. 4 shows that the farther a negative RE ($\lambda < 0$) from the imaginary axis, the smaller the delay margin $\tau^* = \frac{\pi}{2|\lambda|}$ is. For this reason, and based on the inequality conditions above, the RE of $\mathcal{Q}(G_3)$, which is one of $\lambda_q[\mathcal{Q}(G_3)]$, corresponds to a smaller delay margin $\tau_{G_3}^*$ compared with $\tau_{G_1}^*$ and $\tau_{G_2}^*$. ■

The proof above states that if all nonzero eigenvalues of both $\mathcal{Q}(G_1)$ and $\mathcal{Q}(G_2)$ are negative real (e.g., the matrices could be symmetric), then we always have $\tau_{G_3}^* < \min\{\tau_{G_1}^*, \tau_{G_2}^*\}$.

We next explore another scenario, where $\mathcal{Q}(G_1)$ has complex conjugate eigenvalues. If $\mathcal{Q}(G_1)$ with $n_1 = 3$ has complex conjugate eigenvalues and $\lambda_1[\mathcal{Q}(G_1)] = 0$, and the nonzero eigenvalues of $\mathcal{Q}(G_2)$ with arbitrarily large n_2 are all negative real, then the delay margin $\tau_{G_3}^*$ can be made as large as $\tau_{G_1}^*$, but $\tau_{G_3}^*$ will still be smaller than $\tau_{G_2}^*$:

(i) The condition $\tau_{G_3}^* = \tau_{G_1}^*$ is justified as follows. Notice that one can find two different complex conjugate eigenvalue locations on the same contour on DMCM, where each conjugate has the same imaginary part indicating that it is possible to shift the complex conjugate eigenvalues away from the imaginary axis using the negative real eigenvalues of $\mathcal{Q}(G_2)$ while keeping τ^* the same.

(ii) To see the validity of $\tau_{G_3}^* < \tau_{G_2}^*$, we again inspect the geometry of the contours on DMCM. Notice that when a pair of complex conjugate eigenvalues $\tilde{\lambda} = \sigma \mp j\omega$ of $\mathcal{Q}(G_1)$ with $\sigma \neq 0$ and $\omega \neq 0$ is shifted away from the imaginary axis using Kronecker summation and by only changing its real part at an amount of $\Delta < 0$, where Δ is the RE of $\mathcal{Q}(G_2)$, then the delay margin corresponding to $\tilde{\lambda} + \Delta$ is always less than the delay margin corresponding to Δ . This is because $\sigma + \Delta$ is always less than Δ , hence Δ always corresponds to a larger delay margin (see DMCM). Due to the specific geometry of the contours on DMCM, it is impossible to generate a counter example.

We further the analysis of $n_1 = 3$, and n_2 is arbitrarily large. The generalization to large n_1 will be discussed separately. Based on the discussions above, we know that it is impossible to achieve $\tau_{G_3}^* > \tau_{G_2}^*$. Therefore, given $\mathcal{Q}(G_1)$, we explore the conditions for achieving $\tau_{G_3}^* = \tau_{G_1}^*$, which requires synthesizing G_2 and/or $\mathcal{Q}(G_2)$. For this, we solve for the unknown RE of $\mathcal{Q}(G_2)$ denoted by $\Delta < 0$. In this setting, the responsible eigenvalues of G_1 and G_3 should satisfy

$$\lambda_{G_1} = \sigma \mp j\omega := \rho_1 e^{j\theta_1}, \quad \lambda_{G_3} = \sigma_x \mp j\omega := \rho_3 e^{j\theta_3} \quad (7)$$

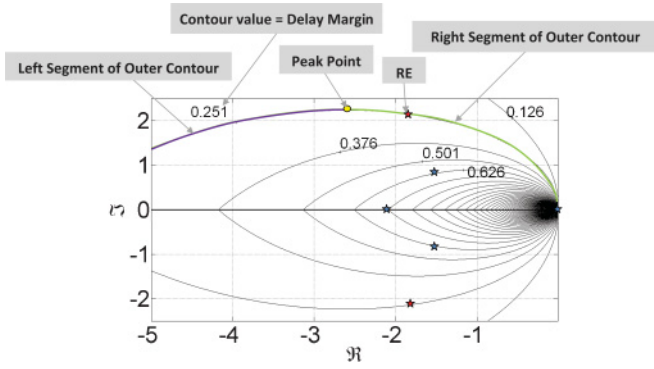


FIG. 6. (Color online) The generic plot that shows the definitions in Definition 2.

where $\sigma_x = \Delta + \sigma$. After some manipulations and noticing the geometric properties in Fig. 1, Eq. (7) leads to

$$\frac{\theta_3 - \frac{\pi}{2}}{\rho_3} = \frac{\theta_1 - \frac{\pi}{2}}{\rho_1}, \quad (8)$$

from which the existence of a feasible solution can be checked. To give an example, let $\sigma = -0.02$ and $\omega = 0.06$. Then the numerical solution of the RE of $Q(G_2)$ and $Q(G_3)$ is obtained, respectively, as $\Delta = \sigma_x - \sigma \approx -0.237$ and $\lambda_{G_3} \approx -0.257 \mp 0.06j$. Using Eq. (5) and these calculated REs, we find $\tau_{G_1}^* = 5.08$, $\tau_{G_2}^* = 8.72$, and $\tau_{G_3}^* = 5.08$. Notice that since Δ is the RE of $Q(G_2)$, it is required that all the other negative real eigenvalues of $Q(G_2)$ should correspond to $\tau_k^* > 8.72$; i.e., these eigenvalues should lie closer to the imaginary axis, in the range of $(-0.237, 0)$. This example supports the claims above, while showing that the largest value that $\tau_{G_3}^*$ can attain

is the delay margin $\tau_{G_1}^*$ found from the complex conjugate eigenvalues $-0.02 \mp 0.06j$ associated with G_1 .

To summarize, it is possible to have $\tau_{G_2}^* > \tau_{G_1}^* \geq \tau_{G_3}^*$ where $n_1 = 3$, n_2 is arbitrarily large, and $n_3 = n_1 \cdot n_2$. This result and the discussions above give the conditions on the graph Laplacians and the limitations on the largest achievable delay margin using Cartesian product. See another study in Ref. [45] on achievable delay margin.

We now discuss how the above properties can be extended to arbitrarily large n_1 and how the delay margin $\tau_{G_3}^*$ is affected. Although we do not provide an exhaustive list of all possible scenarios, the following discussions clearly demonstrate the intricacies of the graph design procedure using DMCM.

Definition 2. In Fig. 6:

Outer contour: The contour on which the RE resides.

Peak point: The point on the outer contour where the positive imaginary part is the maximum.

Left segment of outer contour: The part of the outer contour that starts from the peak point (inclusive) and ends on the negative real axis.

Right segment of outer contour: The part of the outer contour that starts from the peak point (exclusive) and converges to the origin of the complex plane.

Destination contour: The contour on which the RE of $Q(G_3)$ is placed as G_3 is obtained by tailoring G_1 and G_2 via Cartesian product (see Fig. 7).

Consider the two scenarios in two separate columns in Fig. 7. The first one is for having $\tau_{G_3}^* = \tau_{G_1}^*$. By choosing $|\Delta|$ less than or equal to the minimum of the horizontal distance of each eigenvalue of $Q(G_1)$ to the destination contour, we can obtain $\tau_{G_3}^* = \tau_{G_1}^*$ as long as the RE of $Q(G_1)$ lies on the right segment of outer contour. Under this setting, the RE of $Q(G_2)$

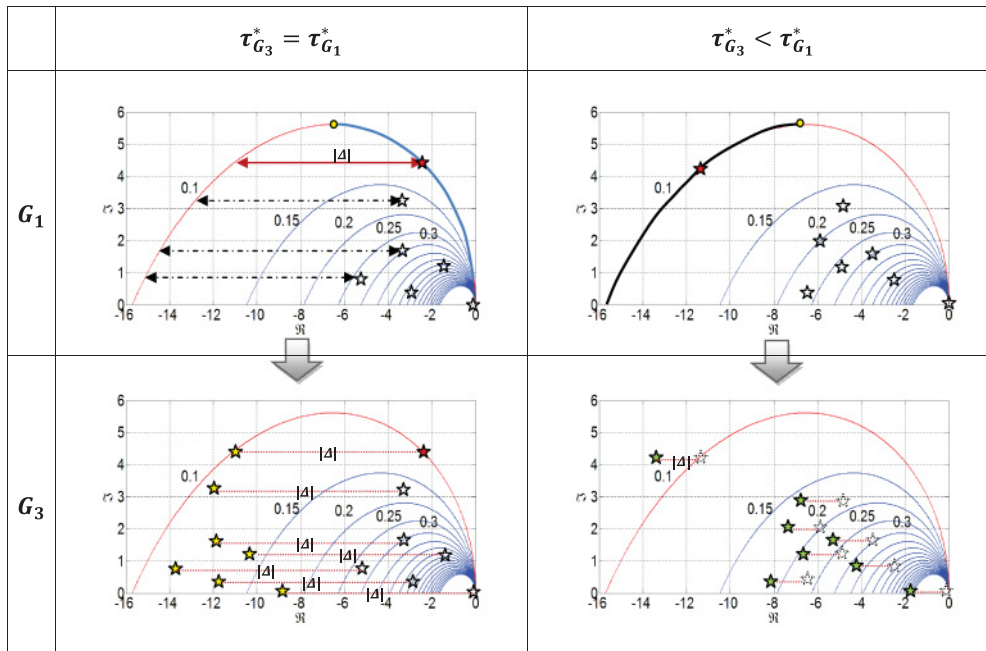


FIG. 7. (Color online) Given nonzero eigenvalues of $Q(G_2)$ are all negative real, one can have several possibilities for $Q(G_1)$ such that $\tau_{G_3}^*$ is either equal to or less than $\tau_{G_1}^*$. Here, we show one scenario for each possibility, where $\tau_{G_1}^* = \tau_{G_3}^*$ is possible if the RE of $Q(G_1)$ lies on the right segment of outer contour and by setting $\min \lambda_{\nu}[Q(G_2)] = \Delta$, where $|\Delta|$ is the shortest distance to the destination contour, and $\tau_{G_1}^* < \tau_{G_3}^*$ occurs if the RE of $Q(G_1)$ lies on the left segment of outer contour.

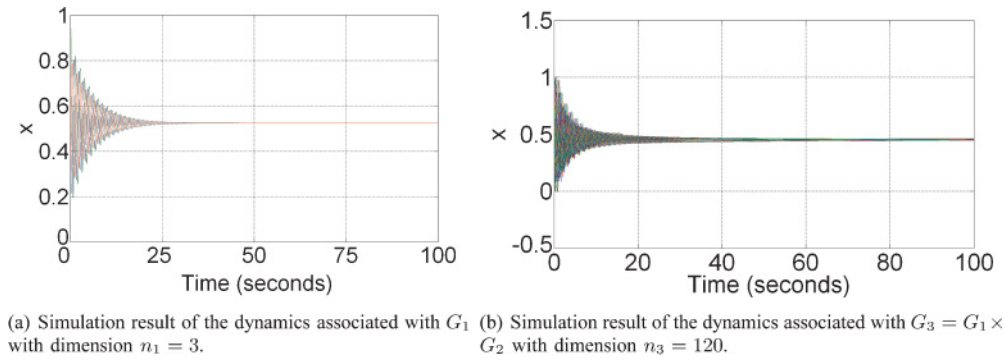


FIG. 8. (Color online) Simulation result of the dynamics associated with G_1 and G_3 show that both dynamics are synchronizable when $\tau = 0.12$. This is because both dynamics can tolerate 0.12 of delay since $\tau_{G_1}^* \approx \tau_{G_3}^* \approx 0.13 > 0.12$.

is Δ , which is the smallest of all the negative real eigenvalues of $\mathcal{Q}(G_2)$. The second scenario is for having $\tau_{G_3}^* < \tau_{G_1}^*$; see Fig. 7. This may occur when the RE of $\mathcal{Q}(G_1)$ lies on the left segment of outer contour and, therefore, as it migrates further to the left, it lands on a contour with a smaller contour value, i.e., smaller delay margin. This scenario is inevitable, no matter how large the negative real eigenvalues of $\mathcal{Q}(G_2)$ are selected.

We next present simulations of a scenario where the number of nodes of G_1, G_2 , and G_3 are, respectively, $n_1 = 3$, $n_2 = 40$, and $n_3 = 3 \cdot 40 = 120$. The nonzero eigenvalues of $\mathcal{Q}(G_1)$ are located at $-3 \pm 4j$, with the corresponding delay margin of $\tau_{G_1}^* \approx 0.13$. The eigenvalues of $\mathcal{Q}(G_2)$ are located in $[-4.27, 0]$, with the corresponding delay margin of $\tau_{G_2}^* \approx 0.367$ due to the RE at -4.27 , and we find that $\tau_{G_3}^* \approx 0.13$. In Figs. 8(a) and 8(b), we show the simulation result of the perturbation dynamics associated with, respectively, G_1 and $G_3 = G_1 \times G_2$, both with a communication delay of $\tau = 0.12$. Since $\tau_{G_3}^* \approx \tau_{G_1}^* \approx 0.13$, which is larger than $\tau = 0.12$, both dynamics are tolerant to τ , as also confirmed by the simulations.

The decay rate of $x_i(t)$, which is outside the scope of this work, is associated with the dominant or rightmost eigenvalues

of the infinite dimensional system in Eq. (3). For the analysis of dominant roots, we refer the readers to Refs. [16,22].

IV. CONCLUSION

Equilibrium behavior of synchronization dynamics of coupled systems with time delay was studied. The bridge between graph structures and the maximum delay the equilibrium dynamics can tolerate before losing synchronizability (stability) is established. It is shown that weak coupling strengths between the connected nodes can increase the delay tolerance of the large-scale network. Moreover, by following certain rules revealed here, and under certain conditions, it is possible to maintain a certain delay margin of the large-scale system by tailoring two subgraphs using Cartesian product operation.

ACKNOWLEDGMENTS

This research has been supported in part by the US National Science Foundation Award ECCS 0901442. R.S. thanks Dr. Maurizio Porfiri at the Polytechnic Institute of New York University for fruitful discussions regarding Fig. 4.

-
- [1] H. G. Enjieu Kadji, J. B. Chabi Orou, and P. Woafu, *Commun. Nonlinear Sci. Numer. Simulat.* **13**, 1361 (2008).
 - [2] A. Arenas, A. Díaz-Guilera, J. Kurths, Y. Moreno, and C. Zhou, *Phys. Rep.* **469**, 93 (2008).
 - [3] F. K. Skinner, H. Bazzazi, and S. A. Campbell, *J. Comput. Neurosci.* **18**, 343 (2005).
 - [4] S. F. Brandt, A. Pelster, and R. Wessel, *Phys. Rev. E* **74**, 036201 (2006).
 - [5] R. Sipahi, F. M. Atay, and S.-I. Niculescu, *SIAM J. Appl. Math.* **68**, 738 (2007).
 - [6] D. Helbing, *Rev. Mod. Phys.* **73**, 1067 (2001).
 - [7] M. Bando, K. Hasebe, K. Nakanishi, and A. Nakayama, *Phys. Rev. E* **58**, 5429 (1998).
 - [8] R. Sipahi, S. Lämmer, D. Helbing, and S.-I. Niculescu, *ASME J. Dynamic Syst. Measure. Control* **131**, 021005 (2009).
 - [9] P. M. Gade, H. A. Cerdeira, and R. Ramaswamy, *Phys. Rev. E* **52**, 2478 (1995).
 - [10] P. M. Gade, *Phys. Rev. E* **54**, 64 (1996).
 - [11] L. M. Pecora and T. L. Carroll, *Phys. Rev. Lett.* **80**, 2109 (1998).
 - [12] K. S. Fink, G. Johnson, T. Carroll, D. Mar, and L. Pecora, *Phys. Rev. E* **61**, 5080 (2000).
 - [13] J. Jost and M. P. Joy, *Phys. Rev. E* **66**, 036126 (2002).
 - [14] M. Porfiri and F. Fiorilli, *Chaos Solitons Fractals* **41**, 245 (2009).
 - [15] D. Hunt, G. Korniss, and B. K. Szymanski, *Phys. Rev. Lett.* **105**, 068701 (2010).
 - [16] S. Hod, *Phys. Rev. Lett.* **105**, 208701 (2010).
 - [17] N. Abaid and M. Porfiri, *IEEE Trans. Auto. Control* **56**, 649 (2011).
 - [18] R. Olfati-Saber and R. M. Murray, *IEEE Trans. Auto. Control* **49**, 1520 (2004).
 - [19] F. M. Atay and T. Biyikoglu, *Phys. Rev. E* **72**, 016217 (2005).
 - [20] R. Merris, *Linear Alg. Appl.* **197-198**, 143 (1994).
 - [21] F. Chung, *Spectral Graph Theory* (American Mathematical Society, 1997).
 - [22] R. Sipahi, S.-I. Niculescu, C. T. Abdallah, W. Michiels, and K. Gu, *IEEE Control Syst. Mag.* **31**, 38 (2011).

- [23] J. K. Hale and S. M. Verduyn Lunel, *Introduction to Functional Differential Equations* (Springer-Verlag, Berlin, 1993).
- [24] W. Michiels and S.-I. Niculescu, in *Stability and Stabilization of Time-Delay Systems. An Eigenvalue-Based Approach*, Vol. 12 (SIAM, Philadelphia, 2007).
- [25] K. Gu, S.-I. Niculescu, and J. Chen, *J. Math. Anal. Appl.* **311**, 231 (2005).
- [26] N. Olgac and R. Sipahi, *IEEE Trans. Auto. Control* **47**, 793 (2002).
- [27] K. L. Cooke and P. van den Driessche, *Funkcialaj Ekvacioj* **29**, 77 (1986).
- [28] J. E. Marshall, H. Górecki, K. Walton, and A. Korytowski, *Time-Delay Systems: Stability and Performance Criteria with Applications* (Ellis Horwood, New York, 1992).
- [29] S. Nosrati, M. Shafiee, and M. B. Menhaj, *Control Theory Appl. IET* **3**, 1499 (2009).
- [30] W. Ren, R. W. Beard, and E. M. Atkins, *American Control Conference* (Portland, OR, 2005).
- [31] J. A. Fax and R. M. Murray, *IEEE Trans. Auto. Control* **49**, 1465 (2004).
- [32] A. Schöllig, U. Münz, and F. Allgöwer, in *Proceedings of the European Control Conference* (Kos, Greece, 2007), pp. 1197–1202.
- [33] R. Sipahi and W. Qiao, *Control Theory Appl. IET* **5**, 622 (2011).
- [34] R. Olfati-Saber, *Proceedings of the American Control Conference* (Portland, OR, 2005).
- [35] D. Hunt, G. Korniss, and B. K. Szymanski, *Phys. Lett. A* **375**, 880 (2011).
- [36] W. Qiao and R. Sipahi, *ASME Dynamic Systems and Control Conference* (Cambridge, MA, 2010).
- [37] R. Sipahi and S.-I. Niculescu, in *Deterministic Time-Delayed Traffic Flow Models: A Survey* (Springer-Verlag, Berlin, 2010), pp. 297–322.
- [38] J. Lu, D. W. C. Ho, and J. Kurths, *Phys. Rev. E* **80**, 066121 (2009).
- [39] B. Kelleher, C. Bonatto, P. Skoda, S. P. Hegarty, and G. Huyet, *Phys. Rev. E* **81**, 036204 (2010).
- [40] A. R. Horn and C. Johnson, *Matrix Analysis* (Cambridge University Press, Cambridge, 1985).
- [41] W. Qiao and R. Sipahi, *ASME Dynamic Systems and Control Conference* (Arlington, VA, 2011).
- [42] R. A. Horn and C. R. Johnson, *Topics in Matrix Analysis* (Cambridge University Press, Cambridge, 1994).
- [43] S. Geršgorin, in *Bulletin de l'Académie des Sciences de l'URSS. Classe des sciences mathématiques et naturelles*, No. 6, pp. 749–754 (1931).
- [44] R. Sipahi, S.-I. Niculescu, C. T. Abdallah, W. Michiels, and K. Gu, *IEEE Control Syst. Mag.* **31**, 38 (2011).
- [45] R. Middleton and D. Miller, *IEEE Trans. Auto. Control* **52**, 1194 (2007).